Interaction Networks Obtained From Coevolutionary Data Highlight Key Residues across Protein Families: the Case of the G-protein Coupled Receptors

Filippo Baldessari[a] , Riccardo Capelli[b,c], Alejandro Giorgetti[a,b], Paolo Carloni[b]

[a] *Department of Biotechnology, University of Verona, Ca' Vignal 1, strada Le Grazie 15, I-37134 Verona, Italy*

[b] *Computational Biomedicine Section, IAS-5/INM-9, Forschungzentrum Juelich, Wilhelm-Johnen-straße, D-52425 Juelich, Germany*

[c] *Present Address: Department of Applied Science and Technology (DISAT), Politecnico di Torino, Corso Duca degli Abruzzi 24, I-10129 Torino, Italy*

Table 1 SI. *Hotspots for each of the structures analysed in the active and inactive states respectively. SeqPos indicates the residue number; BWPos, indicates the Ballesteros-Weinstein position. Highlighted positions are functional: orange highlighting represents positions in contact with ligand binding.*

5HT1B_HUMAN							
Active State				Inactive State			
SeqPos:	BWPos:	AA:	Source:	SeqPos:	BWPos:	AA:	Source:
129	3x32	**D**	[4][5]	53	1x36	**V**	
134	3x37	**T**		95	2x50	**D**	[3]
137	3x40	**I**	[1][2]	96	2x51	**L**	
141	3x44	**C**	[2]	106	2x60	**I**	
212	5x43	**T**		129	3x32	**D**	[4][5]
				132	3x35	**C**	
				133	3x36	**C**	[4][5][6]
				134	3x37	**T**	
				136	3x39	**S**	[3]
				141	3x44	**C**	[2]
				147	3x50	**R**	[1][3]
				180	4x56	**I**	
				208	5x39	**T**	
				212	5x43	**T**	
				224	5x54	**L**	
				227	5x57	**L**	[8]
				309	6x30	**E**	[1]
				317	6x38	**G**	
				324	6x45	**I**	

5HT2A_HUMAN							
Active State				Inactive State			
SeqPos:	BWPos:	AA:	Source:	SeqPos:	BWPos:	AA:	Source:
120	2x50	D	[3]	120	2x50	D	[3]
131	2x60	V		128	2x57	V	[10]
139	Loop	Y		160	3x37	T	
158	3x35	F		162	3x39	S	[3]
160	3x37	T		165	3x42	H	
162	3x39	S	[3]	170	3x47	S	
166	3x43	L	[3]	173	3x50	R	[1][3]
173	3x50	R	[1][3]				
257	5x61	T					
332	6x44	F	[3]				

5HT2B_HUMAN							
Active State				Inactive State			
SeqPos:	BWPos:	AA:	Source:	SeqPos:	BWPos:	AA:	Source:
65	1x43	I		70	1x48	G	
75	1x53	V	[8]	93	2x43	L	[6]
100	2x50	D	[3]	100	2x50	D	[3]
136	3x33	V	[4][5]	104	2x54	I	
140	3x37	T		108	2x57	V	[10]
142	3x39	S	[3]	113	2x62	L	
144	3x41	M		121	Loop	W	
221	5x43	S		131	3x28	W	
240	5x61	T		142	3x39	S	[3]
316	6x27	I		144	3x41	M	
318	6x29	N		149	3x46	I	[8]
322	6x33	A		153	3x50	R	[1][3]
344	6x55	N	[4,5]	157	3x54	I	
374	7x47	G		236	5x57	T	[8]
				319	6x30	E	[1]
				322	6x33	A	
				374	7x47	G	
				384	8x47	N	
				394	8x57	I	

5HT2C_HUMAN							
Active State				Inactive State			
SeqPos:	BWPos:	AA:	Source:	SeqPos:	BWPos:	AA:	Source:
99	2x50	D	[3]	134	3x32	D	[4][5]
134	3x32	D	[4][5]	139	3x37	T	
139	3x37	T		144	3x42	H	
141	3x39	S	[3]				
144	3x42	H					
209	Loop	L					
320	6x44	F	[3]				

AA1R_HUMAN							
Active State				Inactive State			
SeqPos:	BWPos:	AA:	Source:	SeqPos:	BWPos:	AA:	Source:
92	3x37	**Q**		92	3x37	**Q**	
94	3x39	**S**	[3]	94	3x39	**S**	[3]
99	3x44	**L**	[2]				
139	4x57	**G**					
199	5x57	**I**	[8]				

AA2AR_HUMAN							
Active State				Inactive State			
SeqPos:	BWPos:	AA:	Source:	SeqPos:	BWPos:	AA:	Source:
20	1x46	**A**		89	3x37	**Q**	[1]
49	2x47	**A**		91	3x39	**S**	[3]
63	2x60	**F**		93	3x41	**F**	
89	3x37	**Q**	[1]	97	3x45	**A**	
91	3x39	**S**	[3]	102	3x50	**R**	[1][3]
93	3x41	**F**					
102	3x50	**R**	[1][3]				
129	4x50	**W**	[1]				
172	Loop	**V**					
283	7x48	**V**					
290	7x55	**Y**					
299	8x54	**F**					

ACM1_HUMAN							
Active State				Inactive State			
SeqPos:	BWPos:	AA:	Source:	SeqPos:	BWPos:	AA:	Source:
36	1x43	**S**		64	2x43	**L**	[6]
43	1x50	**N**		71	2x50	**D**	[3]
59	2x38	**V**		78	2x56	**F**	
71	2x50	**D**	[3]	106	3x33	**Y**	[4][5]
78	2x56	**F**		114	3x41	**M**	
101	3x28	**W**		123	3x50	**R**	[1][3]
102	3x29	**L**		366	6x36	**T**	
106	3x33	**Y**	[4][5]	367	6x37	**L**	[8]
110	3x37	**N**		412	7x47	**T**	
114	3x41	**M**		414	7x49	**N**	[3]
123	3x50	**R**	[1][3]				
367	6x37	**L**	[8]				
385	6x55	**V**	[4][5]				
412	7x47	**T**					
414	7x49	**N**	[3]				
418	7x53	**Y**	[1]				

ACM2_HUMAN							
Active State				Inactive State			
SeqPos:	BWPos:	AA:	Source:	SeqPos:	BWPos:	AA:	Source:
45	1x54	**M**		69	2x50	**D**	[3]
58	2x39	**N**		77	2x57	**S**	[10]
69	2x50	**D**	[3]	99	3x28	**W**	
77	2x57	**S**	[10]	105	3x34	**V**	
81	2x61	**Y**		110	3x39	**S**	[3]
100	3x29	**L**		113	3x42	**N**	
108	3x37	**N**		118	3x47	**S**	
110	3x39	**S**	[3]	121	3x50	**R**	[1][3]
115	3x44	**L**	[2]	210	5x62	**S**	[8]
147	4x49	**A**					
177	Loop	**Q**					
392	6x40	**I**	[3]				
436	7x49	**N**	[3]				

ACM4_HUMAN							
Active State				Inactive State			
SeqPos:	BWPos:	AA:	Source:	SeqPos:	BWPos:	AA:	Source:
54	1x54	**M**		54	1x54	**M**	
86	2x57	**S**	[10]	78	2x50	**D**	[3]
88	2x59	**N**		86	2x57	**S**	[10]
106	3x26	**D**		88	2x59	**N**	
117	3x37	**N**		130	3x50	**R**	[1][3]
119	3x39	**S**	[3]	401	6x36	**T**	
120	3x40	**V**	[1][2]	449	7x49	**N**	[3]
125	3x45	**I**					
130	3x50	**R**	[1][3]				
165	4x58	**A**					
391	6x26	**M**					
396	6x31	**R**					
401	6x36	**T**					
405	6x40	**I**	[3]				
438	7x37	**I**					
447	7x47	**T**					

ADRB2_HUMAN							
Active State				Inactive State			
SeqPos:	BWPos:	AA:	Source:	SeqPos:	BWPos:	AA:	Source:
47	1x46	**I**		87	2x57	**V**	[10]
87	2x57	**V**	[10]	91	2x61	**G**	
91	2x61	**G**		116	3x35	**C**	
116	3x35	**C**		122	3x41	**E**	
122	3x41	**E**		126	3x45	**V**	
158	4x50	**W**	[1]	131	3x50	**R**	[1][3]
265	6x27	**C**		158	4x50	**W**	[3]
274	6x36	**T**		229	5x68	**Q**	

277	6x39	**I**		268	6x30	**E**	[1]
285	6x47	**C**		272	6x34	**L**	
321	7x48	**F**		285	6x47	**C**	
				321	7x48	**F**	

AGTR1_HUMAN							
Active State				**Inactive State**			
SeqPos:	BWPos:	AA:	Source:	SeqPos:	BWPos:	AA:	Source:
101	3x25	**C**	[5][7]	67	2x43	**L**	[6]
110	3x34	**F**		74	2x50	**D**	[3]
112	3x36	**L**		101	3x25	**C**	[5][7]
115	3x39	**S**	[3]	106	3x30	**A**	
117	3x41	**F**		110	3x34	**F**	
118	3x42	**L**		111	3x35	**N**	
123	3x47	**S**		112	3x36	**L**	
163	4x61	**I**		117	3x41	**F**	
199	5x43	**N**		118	3x42	**L**	
				123	3x47	**S**	
				159	4x56	**A**	
				163	4x61	**I**	
				199	5x43	**N**	
				214	5x57	**S**	[8]
				241	6x36	**I**	
				245	6x40	**I**	[3]
				298	7x49	**N**	[3]

APJ_HUMAN							
Active State				**Inactive State**			
SeqPos:	BWPos:	AA:	Source:	SeqPos:	BWPos:	AA:	Source:
75	2x50	**D**	[3]	75	2x50	**D**	[3]
105	3x28	**S**		105	3x28	**S**	
109	3x32	**I**	[4][5]	109	3x32	**I**	[4][5]
112	3x35	**N**		112	3x35	**N**	
113	3x36	**M**		113	3x36	**M**	
116	3x39	**S**	[3]	116	3x39	**S**	[3]
				118	3x41	**F**	
				119	3x42	**C**	
				122	3x45	**G**	
				124	3x47	**S**	
				257	6x44	**F**	[3]
				260	6x47	**C**	
				296	7x39	**T**	[4][5]
				305	7x49	**N**	[3]
				313	8x47	**D**	

CCR1_HUMAN							
Active State				**Inactive State**			
SeqPos:	BWPos:	AA:	Source:	SeqPos:	BWPos:	AA:	Source:

none	none	none		55	1x53	**V**	[8]
				86	2x56	**T**	
				93	2x63	**Y**	
				116	3x35	**G**	
				123	3x44	**I**	[2]
				154	4x46	**S**	
				158	4x50	**W**	[1]
				211	5x50	**P**	[3]
				259	6x55	**I**	[4][5]

CCR2_HUMAN							
Active State				**Inactive State**			
SeqPos:	BWPos:	AA:	Source:	SeqPos:	BWPos:	AA:	Source:
none	none	none	none	81	2x43	**L**	[6]
				94	2x56	**T**	
				123	3x35	**G**	
				130	3x42	**F**	
				202	5x39	**T**	

CCR3_HUMAN							
Active State				**Inactive State**			
SeqPos:	BWPos:	AA:	Source:	SeqPos:	BWPos:	AA:	Source:
none	none	none	none	72	2x42	**Y**	
				73	2x43	**L**	[6]
				90	2x46	**L**	[3]
				112	Loop	**F**	
				113	Loop	**Y**	
				114	Loop	**H**	
				116	3x22	**D**	
				123	3x29	**S**	
				131	3x37	**Y**	
				154	Loop	**S**	
				158	4x35	**LOOP**	
				165	4x42	**G**	
				197	Loop	**H**	
				202	Loop	**R**	
				215	5x40	**L**	
				234	5x58	**Y**	[1]
				242	5x66	**L**	
				247	Loop	**V**	
				284	6x65	**F**	
				293	7x28	**S**	

CCR5_HUMAN

Active State				Inactive State			
SeqPos:	BWPos:	AA:	Source:	SeqPos:	BWPos:	AA:	Source:
none	none	none	none	37	1x39	**Y**	
				75	2x49	**S**	[10]
				82	2x56	**T**	
				111	3x35	**G**	
				115	3x39	**G**	
				118	3x42	**F**	
				145	4x42	**G**	
				153	4x50	**W**	[1]
				157	4x54	**V**	
				289	7x45	**A**	

CCR9_HUMAN

Active State				Inactive State			
SeqPos:	BWPos:	AA:	Source:	SeqPos:	BWPos:	AA:	Source:
none	none	none	none	129	3x35	**N**	
				135	3x41	**L**	
				264	6x45	**V**	
				267	6x48	**Q**	
				321	8x47	**G**	

CCRL2_HUMAN

Active State				Inactive State			
SeqPos:	BWPos:	AA:	Source:	SeqPos:	BWPos:	AA:	Source:
none	none	none	none	113	3x35	**G**	
				115	3x37	**Y**	
				118	3x40	**T**	
				119	3x41	**F**	
				293	7x46	**C**	[3]

CNR1_HUMAN

Active State				Inactive State			
SeqPos:	BWPos:	AA:	Source:	SeqPos:	BWPos:	AA:	Source:
163	2x50	**D**	[3]	109	Loop	**M**	
194	3x30	**G**		115	1x31	**Q**	
199	3x35	**S**		147	Loop	**L**	
201	3x37	**T**		163	2x50	**D**	[3]
204	3x40	**V**	[1][2]	192	3x28	**K**	
209	3x45	**L**		194	3x30	**G**	
214	3x50	**R**	[1][3]	196	3x32	**V**	[4][5]
393	7x49	**N**	[3]	201	3x37	**T**	
				203	3x39	**S**	[3]
				204	3x40	**V**	[1][2]
				206	3x42	**S**	
				209	3x45	**L**	

211	3x47	**A**	
214	3x50	**R**	[1][3]
215	3x51	**Y**	[8]
270	Loop	**H**	
304	5x68	**H**	
338	6x30	**D**	[1]
339	6x31	**I**	
352	6x44	**L**	
356	6x48	**W**	[3][4][5]
357	6x49	**G**	
358	6x50	**P**	
379	7x34	**V**	
382	7x37	**F**	
406	8x52	**H**	

CNR2_HUMAN

Active State				Inactive State			
SeqPos:	BWPos:	AA:	Source:	SeqPos:	BWPos:	AA:	Source:
80	2x50	**D**	[3]	73	2x43	**I**	[6]
87	2x57	**F**	[10]	78	2x48	**G**	
117	3x36	**F**	[4][5][6]	86	2x56	**V**	
122	3x41	**G**		87	2x57	**F**	[10]
128	3x47	**A**		127	3x46	**T**	[8]
209	5x58	**Y**	[1]	131	3x50	**R**	[1][3]
214	5x63	**W**		247	6x37	**L**	[8]
				248	6x38	**G**	
				258	6x48	**W**	[3][4][5]
				303	8x47	**S**	

DRD2_HUMAN

Active State				Inactive State			
SeqPos:	BWPos:	AA:	Source:	SeqPos:	BWPos:	AA:	Source:
48	1x46	**I**		117	3x35	**M**	
117	3x35	**M**		119	3x37	**T**	
119	3x37	**T**		121	3x39	**S**	[3]
124	3x42	**N**		124	3x43	**L**	[3]
193	5x43	**S**		126	3x44	**C**	[2]
208	5x57	**V**	[8]	129	3x47	**S**	
377	6x39	**I**		132	3x50	**R**	[1][3]
421	7x48	**V**		193	5x43	**S**	
429	7x56	**F**		205	5x54	**T**	
				208	5x57	**V**	[8]
				368	6x30	**E**	[1]
				383	6x45	**I**	
				409	7x35	**Y**	[4][5]

DRD3_HUMAN							
Active State				Inactive State			
SeqPos:	BWPos:	AA:	Source:	SeqPos:	BWPos:	AA:	Source:
75	2x50	D	[3]	68	2x43	V	[6]
115	3x37	T		75	2x50	D	[3]
117	3x39	S	[3]	83	2x57	V	[10]
120	3x42	N		90	2x64	L	
124	3x46	I	[8]	115	3x37	T	
125	3x47	S		117	3x39	S	[3]
153	4x45	M		120	3x42	N	
204	5x54	T		124	3x46	I	[8]
206	5x56	L		125	3x47	S	
207	5x57	V	[8]	128	3x50	R	[1][3]
211	5x61	I		192	5x43	S	
324	6x30	E	[1]	207	5x57	V	[8]
327	6x33	A		324	6x30	E	[1]
339	6x45	I		335	6x41	L	[3]
343	6x49	L		339	6x45	I	
366	7x35	Y	[4][5]	366	7x35	Y	[4][5]
379	7x49	N	[3]				

DRD4_HUMAN							
Active State				Inactive State			
SeqPos:	BWPos:	AA:	Source:	SeqPos:	BWPos:	AA:	Source:
45	1x43	I		56	1x54	C	
48	1x46	V		73	2x43	I	[6]
81	2x51	L		80	2x50	D	[3]
87	2x56	L		88	2x57	V	[10]
88	2x57	V	[10]	108	3x25	C	[5][7]
116	3x33	V	[4][5]	113	3x30	A	
119	3x36	C	[4][5][6]	118	3x35	L	
120	3x37	T		122	3x39	S	[3]
122	3x39	S	[3]	128	3x45	A	
125	3x42	N		133	3x50	R	[1][3]
211	5x57	L	[8]	160	4x50	W	[1]
442	7x47	A		399	6x40	V	[3]
				407	6x48	W	[3][4][5]
				440	7x45	N	[3]

OPRD_HUMAN							
Active State				Inactive State			
SeqPos:	BWPos:	AA:	Source:	SeqPos:	BWPos:	AA:	Source:
105	2x60	Q		70	1x53	V	[8]
130	3x34	Y		95	2x50	D	[3]
132	3x36	M	[4][5][6]	130	3x34	Y	
134	3x38	T		131	3x35	N	[3]
135	3x39	S	[3]	132	3x36	M	[4][5][6]
136	3x40	I	[1][2]	133	3x37	F	

141	3x45	**M**		135	3x39	**S**	[3]
146	3x50	**R**	[1][3]	217	5x43	**F**	
266	6x40	**V**	[3]	264	6x38	**L**	
273	6x47	**C**		266	6x40	**V**	[3]
274	6x48	**W**	[3][4][5]	273	6x47	**C**	
314	7x49	**N**	[3]	274	6x48	**W**	[3][4][5]
321	7x56	**L**		301	7x35	**L**	[4][5]
322	8x47	**D**		314	7x49	**N**	[3]
				321	7x56	**L**	

OPRK_HUMAN							
Active State				**Inactive State**			
SeqPos:	BWPos:	AA:	Source:	SeqPos:	BWPos:	AA:	Source:
98	2x43	**I**	[6]	98	2x43	**I**	[6]
141	3x35	**N**		105	2x50	**D**	[3]
142	3x36	**M**	[4][5]	135	3x29	**I**	
145	3x39	**S**	[3]	141	3x35	**N**	
286	6x50	**P**		142	3x36	**M**	[4][5]
326	7x49	**N**	[3]	143	3x37	**F**	
				145	3x39	**S**	[3]
				279	6x40	**V**	[3]
				315	7x37	**F**	
				326	7x49	**N**	[3]

OPRX_HUMAN							
Active State				**Inactive State**			
SeqPos:	BWPos:	AA:	Source:	SeqPos:	BWPos:	AA:	Source:
132	3x34	**Y**		90	2x43	**I**	
134	3x36	**M**	[4][5][6]	97	2x50	**D**	
135	3x37	**F**		132	3x34	**Y**	
137	3x39	**S**	[3]	133	3x35	**N**	
139	3x41	**F**		134	3x36	**M**	[4][5][6]
143	3x45	**A**		135	3x37	**F**	
148	3x50	**R**	[1][3]	148	3x50	**R**	[1][3]
182	4x57	**G**		268	6x40	**V**	[3]
276	6x48	**W**	[3][4][5]	276	6x48	**W**	[3][4][5]
315	7x49	**N**	[3]	315	7x49	**N**	[3]

OPSD_HUMAN							
Active State				**Inactive State**			
SeqPos:	BWPos:	AA:	Source:	SeqPos:	BWPos:	AA:	Source:
76	2x43	**L**	[6]	91	2x57	**G**	[10]
116	3x31	**F**		116	3x31	**F**	
118	3x33	**T**	[4][5]	118	3x33	**T**	[4][5]
120	3x35	**G**		120	3x35	**G**	
126	3x41	**W**		126	3x41	**W**	
127	3x42	**S**		127	3x42	**S**	
189	Loop	**I**		189	Loop	**I**	

222	5x57	**C**	[8]	222	5x57	**C**	[8]
227	5x62	**V**	[8]				

	Active state		Inactive State		Both Active & Inactive

	5HT1B	5HT2A	5HT2B	5HT2C	AA1R	AA2AR	ACM1	ACM2	ACM4	ADRB2	AGTR1	APJ	CCR1	CCR2	CCR3	CCR5	CCR9	CCRL2	CNR1	CNR2	DRD2	DRD3	DRD4	OPRD	OPRK	OPRX	OPSD
1.31																											
1.36																											
1.39																											
1.43																											
1.46																											
1.48																											
1.50																											
1.53																											
1.54																											
2.38																											
2.39																											
2.42																											
2.43																											
2.46																											
2.47																											
2.48																											
2.49																											
2.50																											
2.51																											
2.53																											
2.54																											
2.56																											
2.57																											
2.59																											
2.60																											
2.61																											
2.62																											
2.63																											
2.64																											
3.22																											
3.24																											
3.25																											
3.26																											
3.28																											
3.29																											
3.30																											
3.31																											
3.32																											
3.33																											
3.34																											

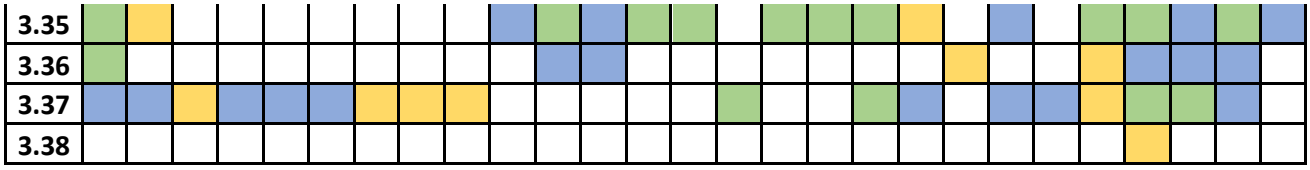
3.35
3.36
3.37
3.38

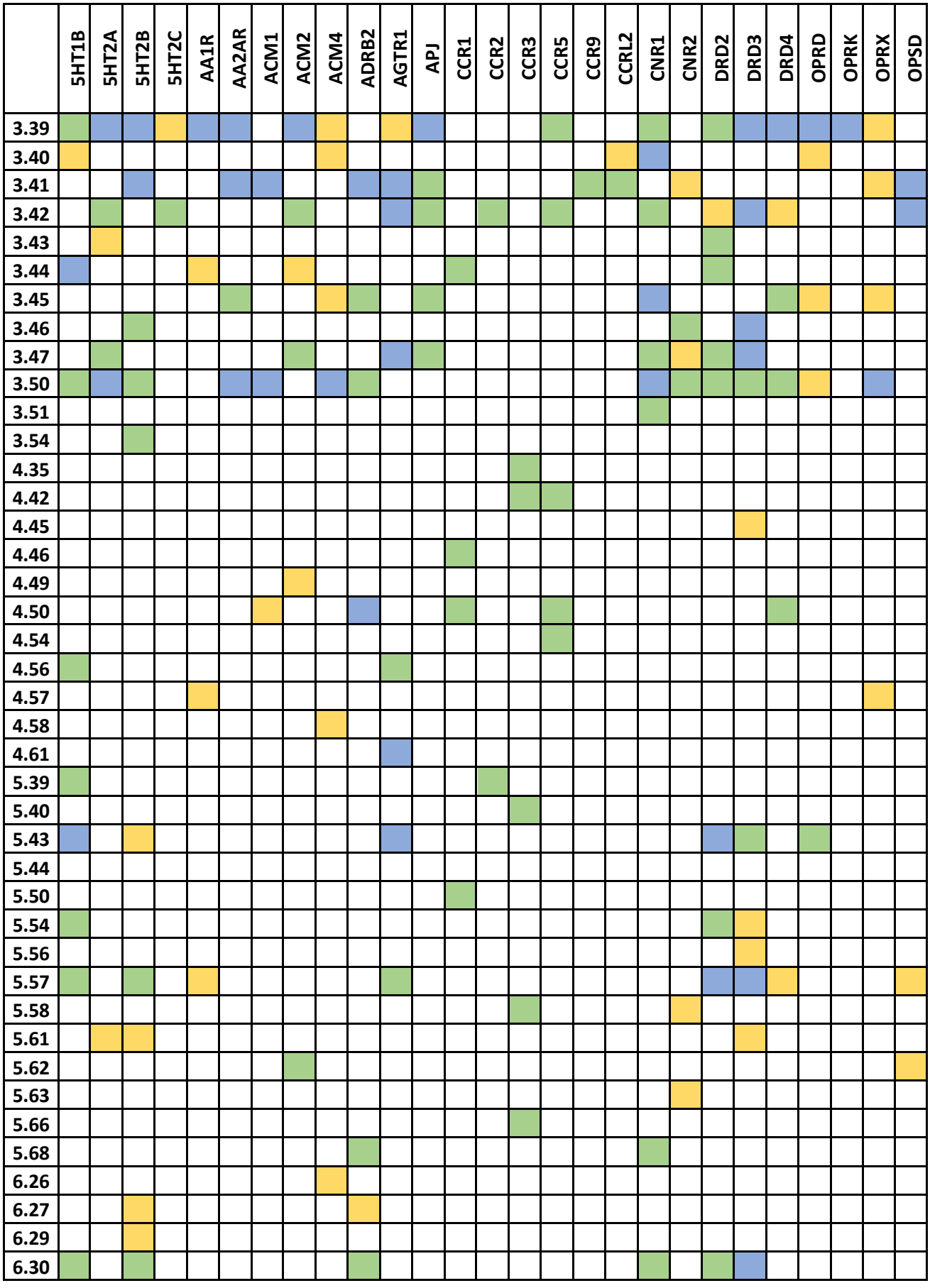
5HT1B
5HT2A
5HT2B
5HT2C
AA1R
AA2AR
ACM1
ACM2
ACM4
ADRB2
AGTR1
APJ
CCR1
CCR2
CCR3
CCR5
CCR9
CCRL2
CNR1
CNR2
DRD2
DRD3
DRD4
OPRD
OPRK
OPRX
OPSD
3.39
3.40
3.41
3.42
3.43
3.44
3.45
3.46
3.47
3.50
3.51
3.54
4.35
4.42
4.45
4.46
4.49
4.50
4.54
4.56
4.57
4.58
4.61
5.39
5.40
5.43
5.44
5.50
5.54
5.56
5.57
5.58
5.61
5.62
5.63
5.66
5.68
6.26
6.27
6.29
6.30

6.31																										
6.33																										

	5HT1B	5HT2A	5HT2B	5HT2C	AA1R	AA2AR	ACM1	ACM2	ACM4	ADRB2	AGTR1	APJ	CCR1	CCR2	CCR3	CCR5	CCR9	CCRL2	CNR1	CNR2	DRD2	DRD3	DRD4	OPRD	OPRK	OPRX	OPSD
6.34																											
6.36																											
6.37																											
6.38																											
6.39																											
6.40																											
6.41																											
6.44																											
6.45																											
6.47																											
6.48																											
6.49																											
6.50																											
6.55																											
6.65																											
7.28																											
7.34																											
7.35																											
7.37																											
7.39																											
7.45																											
7.46																											
7.47																											
7.48																											
7.49																											
7.53																											
7.55																											
7.56																											
8.47																											
8.54																											
8.52																											
8.57																											
Loop															6x				3x								

References:

[1] B. G. Tehan, A. Bortolato, F. E. Blaney, M. P. Weir, J. S. Mason, Unifying family a gpcr theories of activation, Pharmacology & therapeutics 143 (1) (2014) 51-60.

[2] L. Ponzoni, G. Rossetti, L. Maggi, A. Giorgetti, P. Carloni, C. Micheletti, Unifying view of mechanical and functional hotspots across class a gpcrs, PLoS computational biology 13 (2) (2017) e1005381.

[3] V. Katritch, G. Fenalti, E. E. Abola, B. L. Roth, V. Cherezov, R. C. Stevens, Allosteric sodium in class a gpcr signaling, Trends in biochemical sciences 39 (5) (2014) 233-244.

[4] M. Sandal, M. Behrens, A. Brockho, F. Musiani, A. Giorgetti, P. Carloni, W. Meyerhof, Evidence for a transient additional ligand binding site in the tas2r46 bitter taste receptor, Journal of chemical theory and computation 11 (9) (2015) 4439-4449.

[5] E. Suku, A. Giorgetti, Common evolutionary binding mode of rhodopsinlike gpcrs: Insights from structural bioinformatics, AIMS Press, AIMS. Biophysics 4 (2017) 543-556.

[6] B. Trzaskowski, D. Latek, S. Yuan, U. Ghoshdastider, A. Debinski, S. Filipek, Action of molecular switches in gpcrs-theoretical and experimental studies, Current medicinal chemistry 19 (8) (2012) 1090-1109.

[7] M. Wheatley, D. Wootten, M. T. Conner, J. Simms, R. Kendrick, R. T. Logan, D. R. Poyner, J. Barwell, Lifting the lid on gpcrs: the role of extracellular loops. Br J Pharmacol 165 (6) (2012) 1688-1703.

[8] Q. Zhou, D. Yang, M. Wu, Y. Guo, W. Guo, L. Zhong, X. Cai, A. Dai, W. Jang, E. I. Shakhnovich, Z.-J. Liu, R. C. Stevens, N. A. Lambert, M. M. Babu, M.-W. Wang, S. Zhao, Common activation mechanism of class A GPCRs, eLife 8 (2019) e50279.

[9] A. Venkatakrishnan, X. Deupi, G. Lebon, et al. Diverse activation pathways in class A GPCRs converge near the G-protein-coupling region. Nature 536 (2016), 484–487.

[10] A. Schönegge, J. Gallion, L. Picard et al. Evolutionary action and structural basis of the allosteric switch controlling β2AR functional selectivity. Nat Commun 8 (2017), 2169.

Mutation Browser GPCRdb(https://gpcrdb.org/)

Mutagenesis references:

[11] C. Wang,Y. Jiang, J. Ma, H. Wu, D. Wacker, V. Katritch, G. W. Han, W. Liu, X. Huang, E. Vardy, J. D. McCorvy, X. Gao, E. X. Zhou, K. Melcher, C. Zhang, F. Bai, H. Yang, L. Yang, H. Jiang, B. L. Roth, V. Cherezov, R. C. Stevens, H. E. Xu, Structural Basis for Molecular Recognition at Serotonin Receptors. Science 340 (6132) (2013) 610-4.

[12] Sealfon SC, Chi L, Ebersole BJ, Rodic V, Zhang D, Ballesteros JA, Weinstein H., Related contribution of specific helix 2 and 7 residues to conformational activation of the serotonin 5-HT2A receptor. J Biol Chem 270 (28) (1995) 16683-8.

[13] Manivet P, Schneider B, Smith JC, Choi DS, Maroteaux L, Kellermann O, Launay JM., The serotonin binding site of human and murine 5-HT2B receptors: molecular modeling and site-directed mutagenesis. J Biol Chem 277(19) (2002) 17170-8.

[14] John D. McCorvy, Daniel Wacker, Sheng Wang, Bemnat Agegnehu, Jing Liu, Katherine Lansu, Alexandra R. Tribo, Reid H. J. Olsen, Tao Che, Jian Jin & Bryan L. Roth. Structural determinants of 5-HT2B receptor activation and biased agonism. Nat Struct Mol Biol 25(9) (2018) 787-796.

[15] Tania C. Córdova-Sintjago,Yue Liu, Raymond G. Booth, Molecular interactions of agonist and inverse agonist ligands at serotonin 5-HT2C G protein-coupled receptors: computational ligand docking and molecular dynamics studies validated by experimental mutagenesis results, Molecular Physics Volume 113 (3-4) (2015) 348-358.

[16] Peng Y., McCorvy J.D., Harpsøe K., Lansu K., Yuan S., Popov P., Qu L., Pu M., Che T., Nikolajsen L.F., Huang X.P., Wu Y., Shen L., Bjørn-Yoshimoto W.E., Ding K., Wacker D., Han G.W., Cheng J., Katritch V., Jensen A.A., Hanson M.A., Zhao S., Gloriam D.E., Roth B.L., Stevens R.C., Liu Z.J., 5-HT2C Receptor Structures Reveal the Structural Basis of GPCR Polypharmacology. Cell 172 (4) (2018) 719-730.

[17] Rivkees S.A., Barbhaiya H., IJzerman A.P, Identification of the adenine binding site of the human A1 adenosine receptor. J Biol Chem 274 (6) (1999) 3617-21.

[18] Barbhaiya H., McClain R., Ijzerman A., Rivkees S.A., Site-directed mutagenesis of the human A1 adenosine receptor: influences of acidic and hydroxy residues in the first four transmembrane domains on ligand binding. Mol Pharmacol 50 (6) (1996) 1635-42.

[19] Jiang Q., Van Rhee A.M., Kim J., Yehle S., Wess J., Jacobson K.A., Hydrophilic side chains in the third and seventh transmembrane helical domains of human A2A adenosine receptors are required for ligand recognition. Mol Pharmacol 50 (3) (1996) 512-21.

[20] Kim, S.K. et al. Modeling the adenosine receptors: comparison of the binding domains of A2A agonists and antagonists. J Med Chem 46 (23) (2003) 4847-59.

[21] Keov, P. et al. Molecular mechanisms of bitopic ligand engagement with the M1 muscarinic acetylcholine receptor. J Biol Chem 289(34) (2014) 23817-37.

[22] Avlani, V.A. et al. Orthosteric and allosteric modes of interaction of novel selective agonists of the M1 muscarinic acetylcholine receptor.

[23] Bourdon, H. et al. Modelling of the binding site of the human m1 muscarinic receptor: experimental validation and refinement. J Comput Aided Mol 11(4) (1997) 317-32.

[24] Matsui, H. et al. Probing of the location of the allosteric site on m1 muscarinic receptors by site-directed mutagenesis. Mol Pharmacol. 47(1) (1995) 88-98.

[25] Abdul-Ridha, A. et al. Molecular determinants of allosteric modulation at the M1 muscarinic acetylcholine receptor. J Biol Chem 289(9) (2014) 6067-79.

[26] Thal, D.M. et al. Crystal structures of the M1 and M4 muscarinic acetylcholine receptors. Nature 531(7594) (2016) 335-40.

[27] Högger, P. et al. Activating and inactivating mutations in N- and C-terminal i3 loop junctions of muscarinic acetylcholine Hm1 receptors. J Biol Chem270(13) (1995) 7405-10.

[28] Suga, H. et al. Effects of asparagine mutagenesis of conserved aspartic acids in helix 2 (D2.50) and 3 (D3.32) of M1-M4 muscarinic receptors on the irreversible binding of nitrogen mustard analogs of acetylcholine and McN-A-343. Biochemistry 52(29) (2013) 4914-28.

[29] Leppik, R.A. et al. Role of acidic amino acids in the allosteric modulation by gallamine of antagonist binding at the m2 muscarinic acetylcholine receptor. Mol Pharmacol 45(5) (1994) 983-90.

[30] Suga, H. et al. Mutagenesis of nucleophilic residues near the orthosteric binding pocket of M1 and M2 muscarinic receptors: effect on the binding of nitrogen mustard analogs of acetylcholine and McN-A-343. Mol Pharmacol 78(4) (2010) 745-55.

[31] Heitz, F. et al. Site-directed mutagenesis of the putative human muscarinic M2 receptor binding site. Eur J Pharmacol 380(2-3) (1999) 183-95.

[32] Gregory, K.J. et al. Identification of orthosteric and allosteric site mutations in M2 muscarinic acetylcholine receptors that contribute to ligand-selective signaling bias. J Biol Chem 285(10) (2010) 7459-74.

[33] Blüml, K. et al. Functional role of a cytoplasmic aromatic amino acid in muscarinic receptor-mediated activation of phospholipase C. J Biol Chem 269(15) (1994) 11537-41.

[34] Leach, K. et al. The role of transmembrane domain 3 in the actions of orthosteric, allosteric, and atypical agonists of the M4 muscarinic acetylcholine receptor. Mol Pharmacol 79(5) (2011) 855-65.

[35] Zuscik, M.J. et al. Identification of a conserved switch residue responsible for selective constitutive activation of the beta2-adrenergic receptor. J Biol Chem 273(6) (1998) 3401-7.

[36] Dohlman, H.G. et al. Role of extracellular disulfide-bonded cysteines in the ligand binding function of the beta 2-adrenergic receptor. Biochemistry 29(9) (1990) 2335-42.

[37] Javitch, J.A. et al. Constitutive activation of the beta2 adrenergic receptor alters the orientation of its sixth membrane-spanning segment. J Biol Chem 272(30) (1997) 18546-9.

[38] Gether, U. et al. Agonists induce conformational changes in transmembrane domains III and VI of the beta2 adrenoceptor. EMBO J. 16(22) (1997) 6737-47.

[39] Rosenbaum, D.M. et al. GPCR engineering yields high-resolution structural insights into beta2-adrenergic receptor function. Science 318(5854) (2007) 1266-73.

[40] Ghanouni, P. et al. The effect of pH on beta(2) adrenoceptor function. Evidence for protonation-dependent activation. J Biol Chem. 2000 Feb 4;275(5):3121-7.

[41] Hanson, M.A. et al. A specific cholesterol binding site is established by the 2.8 A structure of the human beta2-adrenergic receptor. Structure. 2008 Jun;16(6):897-905.

[42] Jaakola, V.P. et al. The crystallographic structure of the human adenosine A2A receptor in a high-affinity antagonist-bound state: implications for GPCR drug screening and design. Curr Opin Struct Biol. 2010 Aug;20(4):401-14.

[43] Lebon, G. et al. Agonist-bound adenosine A2A receptor structures reveal common features of GPCR activation. Nature. 2011 May 18;474(7352):521-5.

[44] Swaminath, G. et al. Identification of an allosteric binding site for Zn2+ on the beta2 adrenergic receptor. J Biol Chem. 2003 Jan 3;278(1):352-6.

[45] Jensen, A.D. et al. Agonist-induced conformational changes at the cytoplasmic side of transmembrane segment 6 in the beta 2 adrenergic receptor mapped by site-selective fluorescent labeling. J Biol Chem. 2001 Mar 23;276(12):9279-90.

[46] Gouldson. P.R. et al. A new approach to docking in the beta 2-adrenergic receptor that exploits the domain structure of G-protein-coupled receptors. J Med Chem. 1997 Nov 21;40(24):3871-86.

[47] Schneider, E.H. et al. Impact of the DRY motif and the missing "ionic lock" on constitutive activity and G-protein coupling of the human histamine H4 receptor. J Pharmacol Exp Ther. 2010 May;333(2):382-92.

[48] O'Dowd, B.F. et al. Site-directed mutagenesis of the cytoplasmic domains of the human beta 2-adrenergic receptor. Localization of regions involved in G protein-receptor coupling. J Biol Chem. 1988 Nov 5;263(31):15985-92.

[49] Ballesteros, J.A. et al. Activation of the beta 2-adrenergic receptor involves disruption of an ionic lock between the cytoplasmic ends of transmembrane segments 3 and 6. J Biol Chem. 2001 Aug 3;276(31):29171-7.

[50] Sheikh, S.P. et al. Similar structures and shared switch mechanisms of the beta2-adrenoceptor and the parathyroid hormone receptor. Zn(II) bridges between helices III and VI block activation. J Biol Chem. 1999 Jun 11;274(24):17033-41.

[51] Fraser, C.M. Site-directed mutagenesis of beta-adrenergic receptors. Identification of conserved cysteine residues that independently affect ligand binding and receptor activation. J Biol Chem. 1989 Jun 5;264(16):9266-70.

[52] Shi, L. et al. Beta2 adrenergic receptor activation. Modulation of the proline kink in transmembrane 6 by a rotamer toggle switch. J Biol Chem. 2002 Oct 25;277(43):40989-96.

[53] Rasmussen, S.G. et al. Mutation of a highly conserved aspartic acid in the beta2 adrenergic receptor: constitutive activation, structural instability, and conformational rearrangement of transmembrane segment 6. Mol Pharmacol. 1999 Jul;56(1):175-84.

[54] Hines, J. et al. Structural determinants for the activation mechanism of the angiotensin II type 1 receptor differ for phosphoinositide hydrolysis and mitogen-activated protein kinase pathways. Biochem Pharmacol. 2003 Jul 15;66(2):251-62.

[55] Boucard, A.A. et al. Constitutive activation of the angiotensin II type 1 receptor alters the spatial proximity of transmembrane 7 to the ligand-binding pocket. J Biol Chem. 2003 Sep 19;278(38):36628-36. Epub 2003 Jul 3.

[56] Marie, J. et al. Control of conformational equilibria in the human B2 bradykinin receptor. Modeling of nonpeptidic ligand action and comparison to the rhodopsin structure. J Biol Chem. 2001 Nov 2;276(44):41100-11. Epub 2001 Aug 8.

[57] Le, M.T. et al. Angiotensin IV is a potent agonist for constitutive active human AT1 receptors. Distinct roles of the N-and C-terminal residues of angiotensin II during AT1 receptor activation. J Biol Chem. 2002 Jun 28;277(26):23107-10. Epub 2002 May 2.

[58] Perlman, S. et al. Non-peptide angiotensin agonist. Functional and molecular interaction with the AT1 receptor. J Biol Chem. 1995 Jan 27;270(4):1493-6.

[59] Auger-Messier, M. et al. The constitutively active N111G-AT1 receptor for angiotensin II maintains a high affinity conformation despite being uncoupled from its cognate G protein Gq/11alpha. Endocrinology. 2003 Dec;144(12):5277-84. Epub 2003 Aug 13.

[60] Perlman, S. et al. Dual agonistic and antagonistic property of nonpeptide angiotensin AT1 ligands: susceptibility to receptor mutations. Mol Pharmacol. 1997 Feb;51(2):301-11.

[61] Charron, P. et al. Are we ready for pharmacogenomics in heart failure? Eur J Pharmacol. 2001 Apr 6;417(1-2):1-9.

[62] de Mendonça, F.L. et al. Site-directed mutagenesis of CC chemokine receptor 1 reveals the mechanism of action of UCB 35625, a small molecule chemokine receptor antagonist. J Biol Chem. 2005 Feb 11;280(6):4808-16.

[63] Vaidehi, N. et al. Predictions of CCR1 chemokine receptor structure and BX 471 antagonist binding followed by experimental validation. J Biol Chem. 2006 Sep 15;281(37):27613-20.

[64] Garcia-Perez, J. et al. Allosteric model of maraviroc binding to CC chemokine receptor 5 (CCR5). J Biol Chem. 2011 Sep 23;286(38):33409-21.

[65] Dragic, T. et al. A binding pocket for a small molecule inhibitor of HIV-1 entry within the transmembrane helices of CCR5. Proc Natl Acad Sci U S A. 2000 May 9;97(10):5639-44.

[66] Maeda, K. et al. Involvement of the second extracellular loop and transmembrane residues of CCR5 in inhibitor binding and HIV-1 fusion: insights into the mechanism of allosteric inhibition. J Mol Biol. 2008 Sep 12;381(4):956-74. doi: 10.1016/j.jmb.2008.06.041. Epub 2008 Jun 20.

[67] Govaerts, C. et al. The TXP motif in the second transmembrane helix of CCR5. A structural determinant of chemokine-induced activation. J Biol Chem. 2001 Apr 20;276(16):13217-25. Epub 2001 Jan 25.

[68] Murphy, J.W. et al. Integrity of extracellular loop 1 of the human cannabinoid receptor 1 is critical for high-affinity binding of the ligand CP 55,940 but not SR 141716A. Biochem Pharmacol. 2003 May 15;65(10):1623-31.

[69] McAllister, S.D. et al. Cannabinoid receptors can activate and inhibit G protein-coupled inwardly rectifying potassium channels in a xenopus oocyte expression system. J Pharmacol Exp Ther. 1999 Nov;291(2):618-26.

[70] Tao, Q. et al. Mutation of a highly conserved aspartate residue in the second transmembrane domain of the cannabinoid receptors, CB1 and CB2, disrupts G-protein coupling. J Pharmacol Exp Ther. 1998 May;285(2):651-8.

[71] Roche, J.P. et al. A mutation in the second transmembrane region of the CB1 receptor selectively disrupts G protein signaling and prevents receptor internalization. Mol Pharmacol. 1999 Sep;56(3):611-8.

[72] McAllister, S.D. et al. A critical role for a tyrosine residue in the cannabinoid receptors for ligand recognition. Biochem Pharmacol. 2002 Jun 15;63(12):2121-36.

[73] Pan, X. et al. SR 141716A acts as an inverse agonist to increase neuronal voltage-dependent Ca2+ currents by reversal of tonic CB1 cannabinoid receptor activity. Mol Pharmacol. 1998 Dec;54(6):1064-72.

[74] Tao, Q. et al. Role of a conserved lysine residue in the peripheral cannabinoid receptor (CB2): evidence for subtype specificity. Mol Pharmacol. 1999 Mar;55(3):605-13.

[75] Chin, C.N. The third transmembrane helix of the cannabinoid receptor plays a role in the selectivity of aminoalkylindoles for CB2, peripheral cannabinoid receptor. J Pharmacol Exp Ther. 1999 Nov;291(2):837-44.

[76] Song, Z.H. et al. A lysine residue of the cannabinoid receptor is critical for receptor recognition by several agonists but not WIN55212-2. Mol Pharmacol. 1996 May;49(5):891-6.

[77] Hurst, D.P. et al. N-(piperidin-1-yl)-5-(4-chlorophenyl)-1-(2,4-dichlorophenyl)-4-methyl-1H-pyrazole-3-carboxamide (SR141716A) interaction with LYS 3.28(192) is crucial for its inverse agonism at the cannabinoid CB1 receptor. Mol Pharmacol. 2002 Dec;62(6):1274-87.

[78] Latek, D. et al. Modeling of ligand binding to G protein coupled receptors: cannabinoid CB1, CB2 and adrenergic β 2 AR. J Mol Model. 2011 Sep;17(9):2353-66.

[79] Rhee, M.H. et al. Role of the highly conserved Asp-Arg-Tyr motif in signal transduction of the CB2 cannabinoid receptor. FEBS Lett. 2000 Jan 28;466(2-3):300-4.

[80] Mansour, A. et al. Site-directed mutagenesis of the human dopamine D2 receptor. Eur J Pharmacol. 1992 Oct 1;227(2):205-14.

[81] Javitch, J.A. et al. Mapping the binding-site crevice of the dopamine D2 receptor by the substituted-cysteine accessibility method. Neuron. 1995 Apr;14(4):825-31.

[82] Wang, S. et al. Structure of the D2 dopamine receptor bound to the atypical antipsychotic drug risperidone. Nature. 2018 Mar 8;555(7695):269-273.

[83] Javitch, J.A. et al. A cysteine residue in the third membrane-spanning segment of the human D2 dopamine receptor is exposed in the binding-site crevice. Proc Natl Acad Sci U S A. 1994 Oct 25;91(22):10355-9.

[84] Lee, S.P. et al. Inhibition of cell surface expression by mutant receptors demonstrates that D2 dopamine receptors exist as oligomers in the cell. Mol Pharmacol. 2000 Jul;58(1):120-8.

[85] Fowler, J.C. et al. Receptor conformations involved in dopamine D(2L) receptor functional selectivity induced by selected transmembrane-5 serine mutations. Mol Pharmacol. 2012 Jun;81(6):820-31.

[86] Javitch, J.A. A cluster of aromatic residues in the sixth membrane-spanning segment of the dopamine D2 receptor is accessible in the binding-site crevice. Biochemistry. 1998 Jan 27;37(4):998-1006.

[87] Simpson, M.M. et al. Dopamine D4/D2 receptor selectivity is determined by A divergent aromatic microdomain contained within the second, third, and seventh membrane-spanning segments. Mol Pharmacol. 1999 Dec;56(6):1116-26.

[88] Ehrlich, K. et al. Dopamine D2, D3, and D4 selective phenylpiperazines as molecular probes to explore the origins of subtype specific receptor binding. J Med Chem. 2009 Aug 13;52(15):4923-35.

[89] Sartania, N. et al. Role of conserved serine residues in the interaction of agonists with D3 dopamine receptors. J Neurochem. 1999 Jun;72(6):2621-4.

[90] Ferruz, N. et al. Dopamine D3 receptor antagonist reveals a cryptic pocket in aminergic GPCRs. Sci Rep. 2018 Jan 17;8(1):897.

[91] Alberts, G.L. et al. Contributions of cysteine 114 of the human D3 dopamine receptor to ligand binding and sensitivity to external oxidizing agents. Br J Pharmacol. 1998 Oct;125(4):705-10.

[92] Pogozheva, I.D. et al. Opioid receptor three-dimensional structures from distance geometry calculations with hydrogen bonding constraints. Biophys J. 1998 Aug;75(2):612-34.

[93] Chakrabarti, S. et al. The mu-opioid receptor down-regulates differently from the delta-opioid receptor: requirement of a high affinity receptor/G protein complex formation. Mol Pharmacol. 1997 Jul;52(1):105-13.

[94] Petäjä-Repo, U.E. et al. Ligands act as pharmacological chaperones and increase the efficiency of delta opioid receptor maturation. EMBO J. 2002 Apr 2;21(7):1628-37.

[95] Kam, K.W. et al. Constitutive activation of the opioid receptor-like (ORL1) receptor by mutation of Asn133 to tryptophan in the third transmembrane region. J Neurochem. 2002 Dec;83(6):1461-70.

[96] Mouledous, L. et al. Functional inactivation of the nociceptin receptor by alanine substitution of glutamine 286 at the C terminus of transmembrane segment VI: evidence from a site-directed mutagenesis study of the ORL1 receptor transmembrane-binding domain. Mol Pharmacol. 2000 Mar;57(3):495-502.

[97] Neidhardt, J. et al. Different amino acid substitutions at the same position in rhodopsin lead to distinct phenotypes. Invest Ophthalmol Vis Sci. 2006 Apr;47(4):1630-5.

[98] Perez, D.M. et al. Multiple signaling states of G-protein-coupled receptors. Pharmacol Rev. 2005 Jun;57(2):147-61.

[99] Kim, J.M. et al. Structural origins of constitutive activation in rhodopsin: Role of the K296/E113 salt bridge. Proc Natl Acad Sci U S A. 2004 Aug 24;101(34):12508-13.

[100] Iakhine, R. et al. Novel dominant rhodopsin mutation triggers two mechanisms of retinal degeneration and photoreceptor desensitization. J Neurosci. 2004 Mar 10;24(10):2516-26.